A General Rule for Connecting Multiple Multiphase Machines in Series using Phase Transposition

ABBAR SAMIR[1], DEHIBA BOUBAKEUR[1], HOUCINE MILOUDI[2], MOHAMED MILOUDI[2,3], GOURBI ABDELKADER[4], DJERRIRI YOUCEF[1]

[1]IRECOM Laboratory, Electrical Engineering Department,
Djillali Liabes University,
Sidi Bel Abbes,
ALGERIA

[2]APELEC Laboratory, Electrical Engineering Department,
Djillali Liabes University,
Sidi Bel Abbes,
ALGERIA

[3]GIDD Laboratory, Electrical Engineering and Automation Department,
Ahmed Zabana - Relizane University,
Relizane,
ALGERIA

[4]Institute of Science and Applied Techniques,
Ahmed Ben Bella Oran 1 University,
Oran,
ALGERIA

Abstract: - This paper presents a generalized connectivity rule for the serial interconnection of multiple polyphase asynchronous machines, enabling independent torque and flux regulation for each machine via a single voltage inverter. The methodology builds on well-known vector control methods that use Clarke and Park transformations. It also introduces a new phase transposition method that ensures the current components are distributed orthogonally across connected machines. The proposed method is applicable to any N-phase system with an odd number of phases equal to or greater than five, unlike previous studies, which are limited to specific configurations (e.g., five- or eleven-phase systems). This study not only examines the theoretical side of things but also how to put these topologies into practice, with a focus on coordinating phases and separating signals between machines. The suggested method is a scalable and efficient way to handle multimotor drive architectures in situations where the number of converters, wiring complexity, and system reliability are all very important. Simulation examples of five-phase and eleven-phase machines validate the connectivity matrices and demonstrate the versatility of the proposed method.

Key-Words: - Multimotor drives, multiphase machines, Voltage Inverter, Phase Transposition, Clarke–Concordia Transformation, Fortescue Transformation, Electromagnetic interference.

Received: June 15, 2025. Revised: September 28, 2025. Accepted: January 4, 2026. Published: May 29, 2026.

1 Introduction

Since the inception of the first polyphase (five-phase) induction machine in 1969 [1], [2], there has been a marked increase in interest regarding converter-fed polyphase drive systems [3], [4], [5]. A notable characteristic of these machines is that their dynamic modeling results in a formulation in which only two components (α, β; a stationary α-β axis using the Clarke transformation) are directly involved in electromechanical conversion, while the remaining components (x, y, o) represent additional degrees of freedom. This scenario persists even after applying the rotational Park transformation [6].

This transformation facilitates the vector control of torque and flux using only the two components of the stator current axis (d, q), while the axis (x, y) components offer additional degrees of freedom [7]. Consequently, it becomes feasible to connect the stator windings of multiple machines so that one machine perceives the (d, q) components, whereas the others perceive (x, y), thereby enabling independent control of multiple machines using a single voltage inverter [8]. This is accomplished through a specific phase-transposition method that ensures that the same current components do not simultaneously generate torque in multiple machines.

Recent investigations into electromagnetic interference (EMI) [9], [10] and electromagnetic compatibility (EMC) [11], [12] have underscored the importance of precise modeling and mitigation of conducted emissions, particularly in inverter-fed machines [13], [14], [15]. For instance, several studies have concentrated on modeling differential-mode [16], [17] and common-mode [18], [19], [20] impedances in single-phase and three-phase machines [21] to predict EMI behavior and inform filter design [22], [23]. Although most EMC-related research has focused on three-phase systems [24], single-phase [25], [26], and multiphase configurations [27], [28] are gaining relevance due to their application in cost-effective and compact environments, such as household appliances and light-duty industrial machines [29], [30]. Furthermore, high-frequency modeling [31] of AC motors [32], [33], the role of inverter-cable-motor interactions [34], [35], and comparative analysis of EMI [36] behavior in motors [37], [38] provide the foundation for extending the analysis to multiphase [39] multimotor configurations [40], [41]. In addition to these advancements, several recent publications have bolstered research on electrical machines and inverter-fed systems, including multiphase transformer design [29], EMI characterization in converters [36], differential-mode impedance analysis [37], serial connection of induction machines [39], and observer-based control strategies for electrical machines [41]. Moreover, additional studies from 2025 have examined the electromechanical behavior of induction motors [42], stator flux orientation under NPC inverters [43], and dynamic model simulations incorporating real-world measurements in generator systems [44], reflecting ongoing progress in the advanced modeling and control of electric drives. Despite these advancements, the principles of connectivity for arbitrary N-phase systems remain fragmented and unexplored, [45].

The present study seeks to address this gap by establishing a generalized connectivity rule applicable to any number of phases and machines connected in series. This enables the complete and independent control of multiple machines via a single inverter, contributing to both power-electronics design and EMC performance optimization.

The objective of this study is to demonstrate the methodology for calculating the phases to be connected for any N-phase machine. This methodology was subsequently applied to the connection of two machines with five and eleven phases, respectively.

2 System Modeling Tools

2.1 Clarke-Concordia Transformation

Consider a balanced N-phase machine in which the phase windings are uniformly distributed, with each phase shifted by an electrical angle of $\frac{2\pi}{N}$.

To facilitate analysis and enable vector control, it is advantageous to define two orthogonal axes, α and β, within the stationary reference frame, as illustrated in Figure 1.

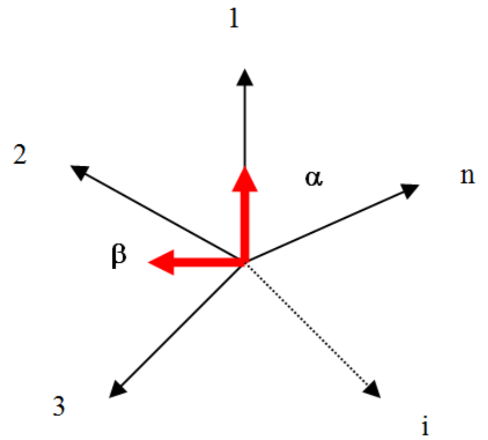

Fig. 1: Flow projection axes
Source: created by the authors

These axes form the foundation of Clarke's (or Concordia) transformation.

The d-axis is aligned with the initial phase, which serves as the reference or origin. To examine the electromechanical behavior of the machine, the magnetic flux produced by each phase winding was projected onto the d-q reference frame. This projection converts the multiphase system into a simplified set of components—typically two active components (d and q) and N−2 zero-sequence or non-sequential components—facilitating efficient torque and flux control.

Let the instantaneous flux vector of the machine be:

$$\Phi(t) = [\Phi_1(t), \Phi_2(t), \dots, \Phi_N(t)]^T \quad (1)$$

where T denotes the transpose.

The flux projections onto the stationary axes α and β are as follows:

$$\begin{cases} \Phi_\alpha = \sum_{i=1}^{i=N} \Phi_i \, cos(\theta_i) \\ \Phi_\beta = \sum_{i=1}^{i=N} \Phi_i \, sin(\theta_i) \end{cases} \quad (2)$$

where θ_i denotes the electrical angle of phase i relative to the reference phase.

When the phases are evenly distributed in space, $\theta_i = i.2\pi/N$, the angular positions can be expressed as:

$$\begin{cases} \Phi_\alpha = \sum_{i=0}^{i=N-1} \Phi_i \, cos(i * 2\frac{\pi}{N}) \\ \Phi_\beta = \sum_{i=0}^{i=N-1} \Phi_i \, sin(i * 2\frac{\pi}{N}) \end{cases} \quad (3)$$

Consequently, the projection vectors α and β in the canonical basis are:

$$\begin{cases} \alpha^t = (1, cos\left(2\frac{\pi}{N}\right), \dots, cos\left((N-1) * 2\frac{\pi}{N}\right) \\ \beta^t = (0, sin\left(2\frac{\pi}{N}\right), \dots, sin\left((N-1) * 2\frac{\pi}{N}\right) \end{cases} \quad (4)$$

The orthogonality of the two projection vectors, denoted as d and q, can be readily verified. Together, these vectors span a two-dimensional subspace known as the Clarke–Concordia plane, also called the electromechanical conversion plane. This plane is particularly significant because only the components projected onto it directly contribute to torque generation. In the specific instance where N=3, this projection simplifies to the classical Clarke transformation.

However, it is important to note that this basis is not inherently normalized. To address this issue, each vector was scaled by a factor $\sqrt{(2/N)}$, facilitating the construction of an orthonormal basis within the Clarke–Concordia plane:

$$\alpha' = \sqrt{\frac{2}{N}}\alpha, \ \beta' = \sqrt{\frac{2}{N}}\beta \quad (5)$$

The complete vector space of the N-phase system is achieved by incorporating N-2 additional orthonormal vectors, which are mutually orthogonal and orthogonal to the α′ and β′ components.

The general method for constructing these vectors is as follows:

<u>“i “is even:</u>

$$e_i = [\cos(0), \cos(i * (\pi/N)), \dots, \cos(i * \left((N-1) * \frac{\pi}{N}\right)] \quad (6)$$

<u>“i “is odd:</u>

$$e_i = [\sin(0), \sin((i+1) * (\pi/N)), \dots, \sin((i+1) * \left((N-1) * \frac{\pi}{N}\right)] \quad (7)$$

In this context, i=0 corresponds to the homopolar vector, while i=1 and i=2 represent the Clarke vectors (α, β). The indices i = =3, …, N−1 are associated with the non-sequential vectors. This configuration yields a comprehensive orthonormal basis for the entire system's state space.

Consequently, the transformation matrix from the phase frame to the Clarke–Concordia frame is established as follows:

$$C = \begin{bmatrix} 1 & \cos\left(\frac{2\pi}{N}\right) & \dots. & \cos\left(\frac{2(N-1)\pi}{N}\right) \\ 0 & \sin\left(\frac{2\pi}{N}\right) & \dots. & \sin\left(\frac{2(N-1)\pi}{N}\right) \\ 1 & \cos\left(2\frac{2\pi}{N}\right) & \dots & \cos\left(2\frac{2(N-1)\pi}{N}\right) \\ 0 & \sin\left(2\frac{2\pi}{N}\right) & \dots. & \sin\left(2\frac{2(N-1)\pi}{N}\right) \\ \frac{\sqrt{2}}{2} & \frac{\sqrt{2}}{2} & \dots.. & \frac{\sqrt{2}}{2} \end{bmatrix} \quad (8)$$

This matrix is orthogonal, meaning that its inverse is simply its transpose. The flux vector in the Clarke–Concordia frame is then obtained as:

$$\Phi_{\alpha,\beta} = C \, \Phi(t) \quad (9)$$

This approach simplifies the N-phase system to a two-dimensional plane (d-q), facilitating straightforward control of torque and flux, while managing higher-order components separately. Upon establishing the orthonormal basis, the corresponding transformation matrices can be systematically constructed using the specified algorithm, thereby ensuring independent control and decoupled representation of all machine components.

2.2 Homopolar and Non-Sequential Components

The components that are orthogonal to the Clarke–Concordia plane can be categorized into two distinct types: homopolar and non-sequential.

2.2.1 Homopolar Component

The homopolar component refers to the scenario in which all phase quantities are identical at any given moment, analogous to the three-phase case (G_a=G_b=G_c).

In an N-phase system, the homopolar current is defined as:

$$i_H(t) = \frac{1}{N}\sum_{k=1}^{N} i_k(t) \quad (10)$$

This corresponds to a vector aligned along the homopolar direction:

$$e_0 = \frac{1}{\sqrt{N}}[1,1, \dots. ,1]^T \quad (11)$$

The projection of the phase current vector *i(t)* onto this homopolar vector yields:

$$i_H(t) = e_0^T i(t) = \frac{1}{\sqrt{N}} \sum_{k=1}^{N} i_k(t) \qquad (12)$$

The homopolar component primarily generates magnetic flux through the machine's leakage paths and does not contribute to net torque.

2.2.2 Non-Sequential Components

In contrast, the non-sequential components are, by design, orthogonal to both the Clarke–Concordia plane vectors (e_α , e_β) and the homopolar direction (e_0).

By definition, the sum of the components of each non-sequential vector is zero:

$$\sum_{k=1}^{N} i_{ns,k}^{(j)}(t) = 0 \qquad (13)$$

Where: $j=1, \ldots, N-3$

Although nonsequential components do not contribute to flux generation or torque production, their presence may still influence system behavior. Ideally, one would remove or suppress these components to simplify control and modeling; however, this process is not straightforward and will be addressed in a subsequent section.

2.2.3 Complete Phase Current Decomposition

Combining all components, the total phase current vector *i(t)* can be decomposed as:

$$i(t) = i_H e_0 + i_\alpha e_\alpha + i_\beta e_\beta + \sum_{j=1}^{N-3} i_{ns}^{(j)} e_{ns}^{(j)} \qquad (14)$$

Where:
i_H: is the homopolar component
i_α, i_β : are the Clarke–Concordia components
$i_{ns}^{(j)}$: are the non-sequential components

This decomposition establishes a comprehensive orthonormal basis for the N-phase system, effectively distinguishing the torque-generating components from those that do not contribute, thereby facilitating systematic analysis and control.

2.3 Park Transform

When a balanced N-phase flux system is projected onto the Clarke–Concordia reference frame (Figure 2), it results in a rotating vector centered at the origin. The corresponding component expressions are:

$$G_{\alpha\beta}(t) = \begin{bmatrix} G_0\cos(\omega t + \phi) \\ G_0\sin(\omega t + \phi) \end{bmatrix} \qquad (15)$$

Where:
G_0: is the amplitude of the rotating vector,
ω: is the electrical angular frequency,
ϕ: is the initial phase.

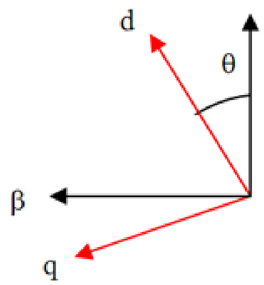

Fig. 2: Park's marker
Source: created by the authors

To facilitate control and analysis, the reference frame was rotated in synchrony with the vector. This was achieved through the application of the Park transformation matrix:

$$P(\theta) = \begin{bmatrix} cos(\theta) & sin(\theta) \\ -sin(\theta) & cos(\theta) \end{bmatrix} \qquad (16)$$

Applying *P(θ)* to the *α-β* components yields the vector in the synchronous rotating frame (*d-q*):

$$G_{dq}(t) = P(\theta) G_{\alpha\beta}(t) = \begin{bmatrix} G_d(t) \\ G_q(t) \end{bmatrix} \qquad (17)$$

Substituting $G_{\alpha\beta}(t)$ from (15):

$$\begin{bmatrix} G_d(t) \\ G_q(t) \end{bmatrix} = \begin{bmatrix} cos(\theta) & sin(\theta) \\ -sin(\theta) & cos(\theta) \end{bmatrix} \begin{bmatrix} G_0\cos(\omega t + \phi) \\ G_0\sin(\omega t + \phi) \end{bmatrix} \qquad (18)$$

By choosing the rotor-aligned angle $\theta = \omega t$, the transformation simplifies to:

$$\begin{bmatrix} G_d(t) \\ G_q(t) \end{bmatrix} = \begin{bmatrix} G_0\cos(\phi) \\ G_0\sin(\phi) \end{bmatrix} \qquad (19)$$

The constant DC values in the d-q frame are derived through the classical Park transformation, which effectively converts sinusoidal AC quantities into DC signals within a synchronous reference frame.

For an N-phase system, the Park transformation can be extended by initially projecting the phase quantities onto the Clarke–Concordia plane as follows:

$$\begin{bmatrix} i_\alpha \\ i_\beta \end{bmatrix} = \begin{bmatrix} \sum_{k=1}^{N} i_k \cos(\theta_k) \\ \sum_{k=1}^{N} i_k \sin(\theta_k) \end{bmatrix}, \quad \theta_k = \frac{2\pi(k-1)}{N} \qquad (20)$$

Then, the same rotation matrix *P(θ)* can be applied to yield the d-q components:

$$i_{dq} = P(\theta) i_{\alpha\beta} \qquad (21)$$

This method effectively reduces the N-phase problem to a two-dimensional synchronous frame, thereby capturing all torque-producing components. In contrast, the remaining N−2 components, which are homopolar and non-sequential, remain orthogonal and do not contribute to torque. Within this transformed frame, the d-axis current component aligns with the magnetic flux, facilitating straightforward field-oriented control, while the q-axis current aligns with torque production. By converting AC quantities to DC values, this approach enables simple PI regulation of both torque and flux, significantly simplifying the overall control strategy.

3 Fortescue Transformation

The concept of symmetrical components was introduced by Fortescue in 1918 as a method for decomposing complex, steady-state phasors [46]. Although originally developed for three-phase systems with sinusoidal time-domain behavior, this technique forms the theoretical foundation for transforming arbitrary instantaneous variables in multiphase systems. Fortescue's method can be generalized to an N-dimensional framework as follows: In this context, we operate within a Hermitian space, where quantities are classically represented in complex exponential form as:

$$\mathrm{G(t)} = \mathrm{G_0 e^{j(\omega t-\phi)}} \tag{22}$$

The present analysis is confined to systems with a prime number of phases, in which the phase displacements are uniformly distributed by 2π/N radians.

For the sake of notational convenience, we define the complex root of unity as $e^{j2\pi/N}$, which functions as a fundamental component in the construction of the transformation matrix.

3.1 Fortescue Base in N Dimension

A unifrequential N-phase system is characterized by 2N degrees of freedom, as each phase vector is defined by both an amplitude and a phase angle.

These two parameters can be effectively combined into a single complex phasor. It can be demonstrated that any N-phase system can be decomposed into symmetrical components, each consisting of vectors with equal magnitudes and uniformly distributed angular separations, along with a single homopolar component, where all phase vectors are in phase. Each component in this decomposition is uniquely defined by its amplitude and phase angle. Within this framework, the concepts of direct and inverse sequences naturally extend to N-dimensional systems. The direct sequence corresponds to a set of vectors that rotate in the same direction as the fundamental system, with successive phases separated by 2π/N.

For a direct symmetrical system, the vector representation is given by:

$$[G_{direct}(\mathrm{t})] = \mathrm{G_0 e^{j(\omega t-\phi)}}\,[1, a^{N-1}, a^{N-2}, \ldots, a^1]^T \tag{23}$$

Similarly, for a reverse system:

$$[G_{inverse}(\mathrm{t})] = \mathrm{G_0 e^{j(\omega t-\phi)}}\,[1, a^1, a^2, \ldots, a^{N-1}]^T \tag{24}$$

Finally, the homopolar (zero-sequence) vector is expressed as follows:

$$[G_{hompolar}(\mathrm{t})] = \mathrm{G_0}\,[1,1,1,\ldots,1]^T \tag{25}$$

Two orthogonal vectors are obtained, typically representing the direct and inverse sequence components. To establish an orthonormal basis, each vector is normalized by multiplying it by the appropriate factor. To complete the basis in an N-dimensional space, it is necessary to define N-2 additional orthogonal vectors. These vectors are constructed to be mutually orthogonal and orthogonal to both the direct and inverse sequences. The general algorithm for constructing a complete set of orthogonal vectors is as follows:

$$e_i = \frac{1}{\sqrt{N}}\,[1, a^i, a^{2i}, \ldots, a^{(N-1)i}]^T \text{ for } i = 0,1,2,\ \ldots\ , N-1 \tag{26}$$

- i=0 → homopolar
- i=1→ inverse sequence
- i=N−1→ direct sequence
- i=2,…,N−2→ non-sequential components

This construction yields a comprehensive orthonormal basis in the Hermitian space, suitable for the symmetrical component analysis of any N-phase system with uniformly spaced phases. However, when N is not a prime number, as exemplified by a six-phase system or a double-star machine, the phase vectors are no longer evenly distributed around the unit circle. This irregularity introduces coupling effects that cannot be fully addressed with a single orthonormal basis derived from the classical root-of-unity method. Instead, such systems can be modeled as a superposition of several subsystems, each possessing a prime number of phases. These subsystems are typically coupled through mutual inductance, particularly in electrical machines. By constructing suitable projection bases for each subsystem, the analytical framework developed for prime-N systems can still be applied, facilitating a piecewise analysis of complex configurations. Based on this, a transformation matrix, often referred to as the passage matrix, can be defined in a manner akin to previous formulations. This matrix is unitary in the Hermitian sense, implying that its inverse can be obtained by taking its conjugate transpose. Such matrices are essential for decomposing and analyzing symmetrical N-phase systems, particularly when N is prime.

3.2 Subsection Vector Properties

Within this framework, the classical components of the three-phase theory are readily identifiable: the homopolar, inverse, and direct vectors. Their fundamental properties align with those observed in the classical context. Specifically:

- The direct vector is responsible for producing useful electromagnetic torque.
- The inverse vector generates torque oscillations or ripples but does not contribute to average torque.
- The homopolar vector does not participate in torque production and generally contributes only to parasitic effects such as leakage flux.

In systems where N > 3, additional vectors beyond the initial three are necessary. These vectors are referred to as nonsequential components. Unlike symmetrical sequences, nonsequential vectors lack a natural order or rotational symmetry. A typical nonsequential system may exhibit a phase order such as 1–4–2–5–3, which does not possess the uniform angular spacing required for the generation of a rotating field:

$$\mathrm{Gns}(t)=\begin{bmatrix} Go\cos(\omega t) \\ Go\cos\left(\omega t-\frac{4\pi}{5}\right) \\ Go\cos\left(\omega t-\frac{8\pi}{5}\right) \\ Go\cos\left(\omega t-\frac{2\pi}{5}\right) \\ Go\cos\left(\omega t-\frac{6\pi}{5}\right) \end{bmatrix} \tag{27}$$

As a result, these components are unable to produce a coherent rotating magnetic field and do not contribute to torque generation. The characterization and potential filtering of these components remain subjects of ongoing research.

3.3 Case of Multi-Frequency Balanced Systems

In the following analysis, we restrict our attention to systems containing harmonic components. Each quantity can thus be expressed as:

$$\overline{G}=\sum_{i=1}^{\infty}\overline{G_i}\,e^{j\omega_i t} \tag{28}$$

The complex phasor, denoted as $\overline{G_\iota}$, represents the harmonic of order i, encompassing both its amplitude and phase. The phase reference is established relative to the fundamental component. From this perspective, the entire system can be interpreted as a superposition of multiple unifrequency subsystems, each corresponding to a specific harmonic order. These harmonic components can be classified into four distinct categories based on their ranks:

- Direct harmonics**:** harmonics of order kN+1
- Inverse harmonics**:** harmonics of order kN−1
- Homopolar harmonics**:** harmonics of order kN
- Non-sequential harmonics**:** all other harmonic orders not fitting the above categories

N denote the number of phases in the system, and k is a non-negative integer.

The classifications are intrinsically linked to the spatial phase progression within each harmonic subsystem. The terminology employed denotes the type of phase sequence generated by each harmonic, which subsequently influences its role in torque production and electromagnetic behavior.

4 Connection Principle of a Polyphase System

The system under examination comprises a polyphase voltage-source inverter operating under pulse-width modulation (PWM) control (Figure 3) and supplying multiple machines connected in series.

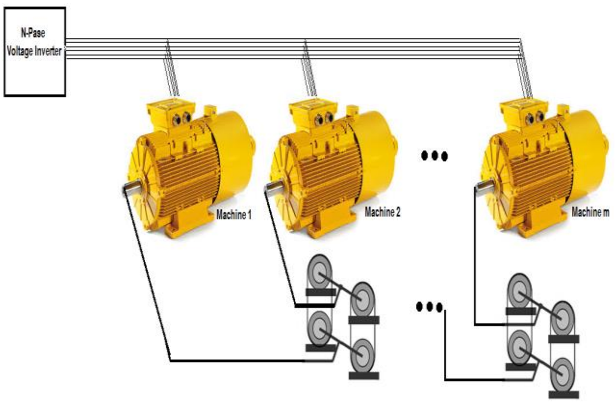

Fig. 3: Block diagram with a proposed command structure
Source: created by the authors

4.1 General Conditions

As established in the preceding sections, the current space of an N-phase system can be decomposed into mutually orthogonal subspaces. Only the components lying in the Clarke–Concordia plane (d,q) contribute to torque production, whereas the nonsequential components (x,y,…) remain orthogonal and do not affect the electromechanical conversion process. This property enables the interconnection of multiple machines in series such that each machine receives a distinct projection of the inverter currents. The key idea is that the stator phases of successive machines must be assigned such that the (d,q) components of one machine map into the non-torque-producing subspaces of the next machine, and vice versa. When this condition is satisfied, each machine operates in an independent vector subspace of the NNN-dimensional current space, enabling full and decoupled control, even though all machines share the same inverter.

For an odd number of phases N, the maximum number of machines that can be connected in this manner is N-1/2.

Figure 4 illustrates this configuration, where (N−1)/2 stator windings are supplied by a single current-controlled N-phase inverter.

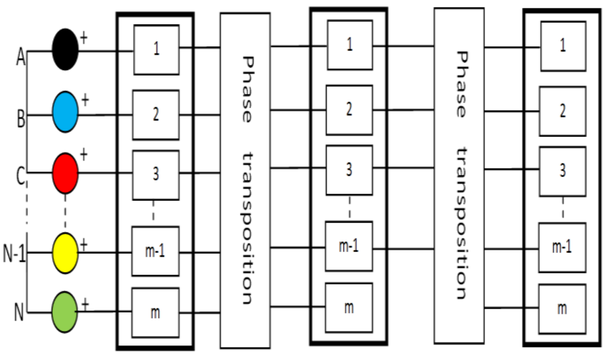

Fig. 4: Series connection of (N−1)/2 machine stator windings powered by an N-phase current-controlled voltage source inverter (assuming N is odd).

Source: created by the authors

The connectivity rule that determines the appropriate phase assignment for each machine is encapsulated in Table 1 and depicted in Figure 5. According to this rule, phase N of one machine is connected to phase N+(N−1) of the subsequent machine, with all indices considered modulo N. This cyclic permutation ensures that each machine perceives a distinct orientation of the Clarke–Concordia plane, thereby receiving orthogonal current components. As a result, the torque and flux can be independently regulated for each machine in the series, without any mutual electromagnetic interference.

Table 1. Connectivity rule for the general N-phase case

Machine	**Phase**
Machine 1	N
Machine 2	N’= N+N-1=N+1*(N-1)
Machine 3	N’’=N’+N-1=N+1*(N-1)+(N-1)=N+2*(N-1)
---	---
Machine m	N’’…’=N+(m-1)*(N-1)

Source: created by the authors

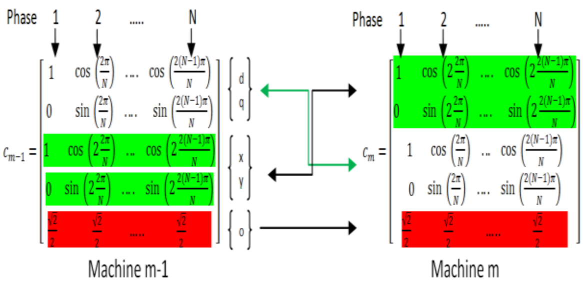

Fig. 5: Principle of connection of two successive machines

Source: created by the authors

This principle serves as the basis for constructing the general phase-transposition rule and the associated connectivity matrices for any odd-phase system with $N \geq 5$.

4.2 Number of Machines to be Connected in Series

This suggests that in a configuration involving (k=(N-1)/2) stator windings from multiphase machines, the interconnection must be arranged such that the current components perceived as – (d-q) by one machine are perceived as – (x-y) components by another, and vice versa. Under these conditions, it becomes feasible to achieve fully independent control of each of the (N-1)/2 machines while the entire drive system is powered by a single current-controlled voltage-source inverter [4].

4.3 The Connection Principle and Connectivity Matrices for any Phase

By decomposing the N-phase system into mutually orthogonal subspaces, such as Clarke–Concordia, Fortescue, and non-sequential components, it becomes feasible to articulate a general connectivity rule. This rule specifies the assignment of stator phases for successive machines when they are connected in series and powered by a single N-phase inverter.

For a given reference phase index N, the phase of the inverter that must be connected to phase i of the m-th machine is obtained from the following relation:

$$N_i = N + (m-1) * (N-1) \qquad (29)$$

Where:

- N_i is the inverter phase number connected to phase i of machine m,
- N is the phase index of the reference phase of the first machine,
- $m \in \{1, 2, \ldots, (N-1)/2\}$ is the machine index in the series connection.

By taking the modulus over N, the phase numbering is cyclically wrapped, ensuring that each machine receives a unique cyclic permutation of the inverter-phase sequence. This phase permutation is crucial for achieving decoupling, as it ensures that the torque-producing current components (d, q) of one machine are transformed into non-torque-producing components (x, y,…) of the subsequent machine, and vice versa. As a result, each machine operates within a distinct orthogonal subspace of the N-dimensional current space.

Consequently, (29) offers a systematic and general rule for constructing the connectivity matrices for any number of machines and any odd-phase configuration, N ≥ 5. This approach obviates the need for case-by-case derivations (such as five-, seven-, and eleven-phase configurations) and extends the method to arbitrary N, thereby facilitating scalable multimotor architectures using a single-voltage inverter.

5 Application on Five-Phase and Eleven-Phase Machines

5.1 Coupling Series Two Five-Phase Machine

Two machines can be connected in series when (k = (5-1)/2).

To facilitate the analysis of this configuration, we employ the following notation: the inverter output voltages are designated with uppercase indices (A, B, C, D, and E), while the phase voltages and currents of the two machines are indicated using lowercase indices (a, b, c, d, and e). The subscript '1' denotes the first machine, and '2' denotes the second machine [8]. With $\alpha = 2\pi/\mathrm{N}$.

.

$$\begin{cases} i_A = i_{a1} = \sqrt{2}I_1 \sin(\omega_1 t) + \sqrt{2}I_2 \sin(\omega_2 t) \\ i_B = i_{b1} = \sqrt{2}I_1 \sin(\omega_1 t - \alpha) + \sqrt{2}I_2 \sin(\omega_2 t - 2\alpha) \\ i_C = i_{c1} = \sqrt{2}I_1 \sin(\omega_1 t - 2\alpha) + \sqrt{2}I_2 \sin(\omega_2 t - 4\alpha) \\ i_D = i_{d1} = \sqrt{2}I_1 \sin(\omega_1 t - 3\alpha) + \sqrt{2}I_2 \sin(\omega_2 t - \alpha) \\ i_E = i_{e1} = \sqrt{2}I_1 \sin(\omega_1 t - 4\alpha) + \sqrt{2}I_2 \sin(\omega_2 t - 3\alpha) \end{cases} \qquad (30)$$

$$\begin{cases} i_A = i_{a2} = \sqrt{2}I_1 \sin(\omega_1 t) + \sqrt{2}I_2 \sin(\omega_2 t) \\ i_{b2} = i_D = \sqrt{2}I_1 \sin(\omega_1 t - 3\alpha) + \sqrt{2}I_2 \sin(\omega_2 t - \alpha) \\ i_{c2} = i_B = \sqrt{2}I \sin(\omega_1 t - \alpha) + \sqrt{2}I_2 \sin(\omega_2 t - 2\alpha) \\ i_{d2} = i_E = \sqrt{2}I_1 \sin(\omega_1 t - 4\alpha) + \sqrt{2}I_2 \sin(\omega_2 t - 3\alpha) \\ i_{e2} = i_C = \sqrt{2}I_1 \sin(\omega_1 t - 2\alpha) + \sqrt{2}I_2 \sin(\omega_2 t - 4\alpha) \end{cases} \qquad (31)$$

The reference currents for the inverter are defined as shown in Table 2 and illustrated in Figure 6.

Table 2. Connectivity matrix, five-phase case

	A	B	C	D	E
M1	1	2	3	4	5
M2	1	3	5	2	4

Source: [6]

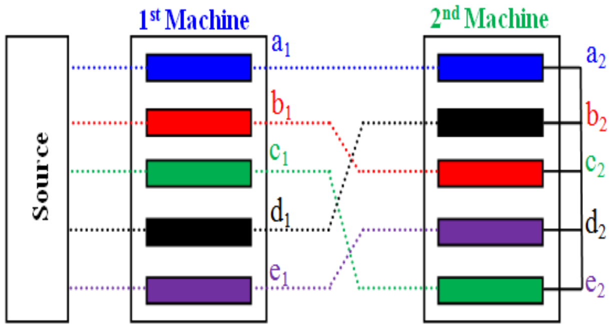

Fig. 6: Connectivity of two five-phase machines
Source: [6]

5.2 Coupling Series Five Eleven-Phase Machine

Five machines can be connected in series when (k = (11-1)/2).

Table 3 delineates the connectivity matrix for a system comprising five eleven-phase asynchronous machines arranged in series. This matrix explicitly specifies the allocation of each inverter output phase to the stator phases of the individual machines, thereby ensuring non-overlapping and orthogonal current paths. Such a configuration enables each machine to operate independently within its own vector subspace while being powered concurrently by a single voltage inverter.

Table 3. Connectivity matrix for the eleven-phase case

	A	B	C	D	E	F	G	H	I	J	K
M1	1	2	3	4	5	6	7	8	9	10	11
M2	1	3	5	7	9	11	2	4	6	8	10
M3	1	4	7	10	2	5	8	11	3	6	9
M4	1	5	9	2	6	10	3	7	11	4	8
M5	1	6	11	5	10	4	9	3	8	2	7

Source: created by the authors

This configuration shown in Figure 7 verifies that phase interleaving has been accurately executed to prevent torque coupling and electromagnetic interactions between the machines. The generalization of this connectivity rule facilitates scalable multimotor architectures and substantiates the theoretical model for any odd-phase configuration, thereby significantly enhancing the applicability of serially connected multiphase-drive systems.

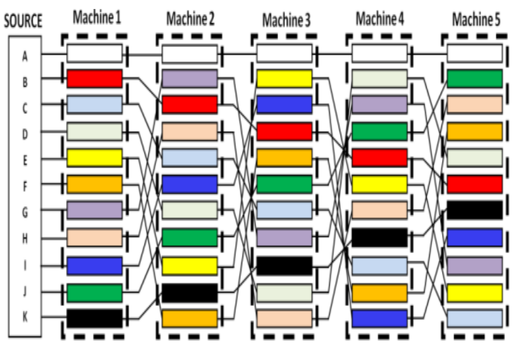

Fig. 7: Connectivity of five eleven-phase machines
Source: created by the authors

The aim of this configuration is to illustrate a viable connection scheme for an eleven-phase machine. The parameter calculations were conducted using the same methodology as that employed for the five-phase machine.

6 Practical Implementation Considerations and Electromagnetic Decoupling in Inverter-Fed Systems

Implementing the proposed connectivity rule in a laboratory setting is relatively straightforward, requiring only precise phase identification and correct wiring in accordance with Equation (29). Minor deviations in stator resistances, leakage inductances, or manufacturing tolerances may slightly affect the ideal orthogonality of the current components; however, these variations can be effectively managed using standard current controllers and conventional measurement equipment. No specialized hardware is required beyond a typical multiphase inverter test bench. In real inverter-fed systems, constraints such as a finite switching frequency, dead-time insertion, and modulation limits introduce minor phase asymmetries. The cyclic phase permutation inherent in the proposed rule distributes these imperfections uniformly among the machines, thereby preventing distortion accumulation and maintaining an effective separation of the current components.

Consequently, the proposed method is fully compatible with standard PWM strategies and commercial inverter hardware. Electromagnetic decoupling occurs because the transposition rule maps the torque-producing (d, q) components of each machine into orthogonal subspaces relative to the other machines. As these subspaces are mutually orthogonal in the Clarke–Concordia and Fortescue representations, their magnetic interactions are negligible to the first order, ensuring that the torque production in one machine does not influence the others. Even when the machines aren't working perfectly, the dominant coupling terms remain small, indicating that the machines act like separate subsystems sharing a single inverter.

7 Conclusion

This research presents a comprehensive theoretical framework for the serial interconnection of multiple N-phase asynchronous machines powered by a singular voltage inverter. This research formulates a generalized connectivity rule applicable to any odd-phase configuration ($N \geq 5$), thereby enhancing existing methodologies previously confined to fixed five-phase or eleven-phase systems. The method uses Clarke–Concordia, Park, and Fortescue transformations to split the current space appropriately, allowing each machine to control torque and flux separately. The connectivity matrices and phase assignment rules ensure that all machines operate in mutually orthogonal subspaces. This stops electromagnetic coupling and unwanted torque interaction.

The analysis of practical implementation aspects, along with the theoretical foundations, shows that the proposed connectivity principle works with standard inverter-fed drive hardware. The method works just as well, even with minor flaws such as phase asymmetries, dead-time effects, and winding tolerances. This is because the cyclic phase permutation evenly distributes these flaws across the machines. This keeps the current components orthogonal and prevents them from interfering with each other, even when in use. So, the suggested method can still be used with standard lab equipment and commercially available multiphase inverters.

The simulation results for both the five-phase and eleven-phase systems confirm the viability, accuracy, and scalability of the proposed interconnection principle. These results show that the proposed method could simplify hardware, make systems more modular, and improve the energy efficiency of multimotor architectures. These architectures are becoming more useful in modern industrial and transportation applications. Future efforts will focus on empirically validating the proposed connectivity rule in actual inverter-machine configurations, evaluating fault-tolerant performance across diverse failure scenarios, and integrating the methodology into real-time control systems for sophisticated applications.

Acknowledgement:
This work was supported by Djillali Liabes University, Sidi Bel Abbes, Algeria.

Declaration of Generative AI and AI-assisted Technologies in the Writing Process
During the preparation of this work the author(s) used Grammarly in order to improve the readability and language of the manuscript. After using this tool, the author(s) reviewed and edited the content as needed and take(s) full responsibility for the content of the publication.

References:

[1] S. Williamson and S. Smith, Pulsating torque and losses in multiphase induction machines, *IEEE Industry Applications*, Vol. 39, No. 4, 2003, pp. 986-993. https://doi.org/10.1109/TIA.2003.813722

[2] G. K. Singh, Multiphase induction machine drive research, *Electric Power Systems Research*, Vol. 61, No. 2, 2002, pp. 139–147. https://doi.org/10.1016/S0378-7796(02)00007-X.

[3] M. J. Bhakti, M. C. Mukul, Two-motor single-inverter field-oriented induction machine drive dynamic performance, *Sadhana Journal*, Vol. 39, No. 2, 2014, pp. 391–407. https://doi.org/10.1007/s12046-014-0237-6.

[4] E. Levi, M. Jones, S. N. Vukosavic and H. A. Toliyat, Operating principles of a novel multiphase multimotor vector-controlled drive, *IEEE Transactions on Energy Conversion*, Vol. 19, No. 3, 2004, pp. 508–516. https://doi.org/10.1109/TEC.2004.832055.

[5] E. Levi, M. Jones, S. N. Vukosavic, A. Iqbal and H. A. Toliyat, Modeling, Control, and Experimental Investigation of a Five-Phase Series-Connected Two-Motor Drive With Single Inverter Supply, *EEE Transactions on Industrial Electronics*, Vol. 54, No. 3, 2007, pp. 1504-1516. https://doi.org/10.1109/TIE.2007.894694.

[6] S. Abbar, K. Fellah, F. Benkhoris, Coupling series two five-phase asynchronous machines powered by a single voltage inverter, *Leonardo Journal of Sciences*, Issue No. 27, 2015, pp. 29–40, [Online]. http://ljs.academicdirect.org/A27/029_040.pdf (Accessed Date: January 10, 2026).

[7] Nacéra Hammadi, Djamel-Eddine Fekir, Saïd Nemmich, Rafik Sayah, Kamel Nassour, Sidi-Mohammed Remaoun, Amar Tilmatine, Experimental analysis of a new separation technique of aluminum/copper particles using a double-side electrostatic actuator, *Journal of Electrostatics*, Vol. 136, 2025. 104098, https://doi.org/10.1016/j.elstat.2025.104098.

[8] D. Kondratenko, A. Lewicki, and K. Łuksza, "Improved speed control of dual induction motor drive powered by a single five-leg voltage source inverter," Scientific Reports, Vol. 15, No. 1, pp. 1–15, 2025, https://doi.org/10.1038/s41598-025-14132-7.

[9] M. Ait Salih, Z. M'barki, Y. Mejdoub, and K. Senhaji Rhazi. Black-box modelling of electromagnetic compatibility in DC–DC converters for electric vehicles, *Acta IMEKO*, vol. 14, no. 2, 2025, pp. 1-8. https://doi.org/10.21014/actaimeko.v14i2.2035.

[10] S. Wang, W. Zhao, X. Zong, and Z. Chen, "Optimal Control Model of Electromagnetic Interference and Filter Design in Motor Drive Systems," Electronics, vol. 14, no. 5, 980, 2025, pp. 1-18 https://doi.org/10.3390/electronics14050980.

[11] S. Yalçın, T. Göksu, S. Kesler, and O. Bingöl, Determination of conducted EMI in SiC based dual active bridge converter, *Int. J. Appl. Methods Electron. Comput.*, vol. 9, pp. 241–

2442025, https://doi.org/10.18100/ijamec.801730.

[12] Z. Wang, D. Jiang, Z. Liu, X. Zhao, G. Yang, and H. Liu, "A Review of EMI Research of High Power Density Motor Drive Systems for Electric Actuator," Actuators, vol. 12, no. 11, 411, 2023, pp. 1-26. https://doi.org/10.3390/act12110411.

[13] P. Babu, Z. Tang, S. Peyghami, F. Blaabjerg, N. Christensen and P. Davari, "Systematic Approach for EMI Equivalent Model Derivation of Three Phase DC-Fed Motor Drives," 2024 International Conference on Electrical Machines (ICEM), Torino, Italy, 2024, pp. 1-7, https://doi.org/10.1109/ICEM60801.2024.10700164.

[14] Y. Hu and X. Chen, "Conductive Common-Mode EMI Suppressing Methods in Inverter-Fed Motor Drives," in Emerging Technologies for Electric and Hybrid Vehicles, Green Energy and Technology, Springer, 2024, pp. 83–114, ISBN 978-981-99-3060-9.

[15] J. Aigner, M. Lemke, T. Dörlemann, and S. Frei, "Broadband Active Common Mode EMI Suppression of a GaN Motor Inverter With Adaptive FIR Filters Using Delay‑Compensated Gate Control Signals," IEEE Trans. Electromagn. Compat., Vol. 67, No. 4, pp. 1213–1227, 2025, https://doi.org/10.1109/TEMC.2025.3582516.

[16] Y. Lai, J. Yao, S. Wang, Z. Luo and Y. Li, "Electric Near Field Emission From a 1Mhz Power Converter For Electric Vehicles, " 2021 IEEE Energy Conversion Congress and Exposition (ECCE), Vancouver, BC, Canada, 2021, pp. 2881-2887. https://doi.org/10.1109/ECCE47101.2021.9595815.

[17] J. Jensen, M. Jensen, L. Nielsen, and K. Pedersen, "Methods for the Investigation and Mitigation of Conducted Differential-Mode Electromagnetic Interference in Commercial Electrical Vehicles," Energies, vol. 18, no. 859, 2025, pp. 1-33. https://doi.org/10.3390/en18040859.

[18] D. Deepankar, T. Ibuchi, and T. Funaki, "Non‑linear Modeling of High-Frequency Differential‑Mode Conducted EMI Emissions in Single‑Phase Inverters," IEEJ Journal of Industry Applications, vol. 14, no. 4, pp. 575–582, 2025, https://doi.org/10.1541/ieejjia.24012531.

[19] A. S. Dickmann and S. Schenke, A novel method of transfer-function identification for modeling differential-mode impedance of AC motors, *International Symposium on Electromagnetic Compatibility - EMC EUROPE, Angers, France*, 2017, pp. 1–5. https://doi.org/10.1109/EMCEurope.2017.8094770.

[20] L. Yang, S. Wang, and J. Feng, Electromagnetic interference modeling and suppression techniques in variable-frequency drive systems, *Front. Mech. Eng.*, vol. 13, no. 3, pp. 329–353, 2018. https://doi.org/10.1007/s11465-018-0466-1

[21] M. Yeshalem, B. Khan, and O. P. Mahela, Conducted electromagnetic emissions of compact fluorescent lamps and electronic ballast modeling, *AIMS Electr. Elect. Eng.*, vol. 6, no. 2, pp. 178–187, 2022. https://doi.org/10.3934/electreng.2022011

[22] D. Zhang, M. Leibl, J. Mühlethaler, J. Huber and J. W. Kolar, "Analytical Modeling and Comparison of EMI pre-filter Noise Emissions of Three-Phase Voltage and Current DC-Link Converters," in IEEE Transactions on Power Electronics, Vol. 39, No. 11, pp. 14691-14707, Nov. 2024. https://doi.org/10.1109/TPEL.2024.3427826.

[23] Y. Moreno, A. Egea, G. Almandoz, G. Ugalde, A. Urdangarin, R. Moreno, High-Frequency Modelling of Electrical Machines for EMC Analysis, *Electronics*, Vol. 13, No. 4, 2024, Article 787, pp. 1–18. https://doi.org/10.3390/electronics13040787.

[24] A. Adam, F. Kacar, C. P. Uzunoglu, Enhancement design of multi-phase transformer for cascaded H-bridge motor driver, *WSEAS Transactions on Circuits and Systems*, Vol. 23, 2024, pp. 165–171. https://doi.org/10.37394/23201.2024.23.17.

[25] Y. Wu, J. Xu, T. B. Soeiro, P. Bauer and Z. Qin, "Frequency Design of Three-Phase Active Front-End Converter With Reduced Filter in EV Chargers," in IEEE Transactions on Transportation Electrification, Vol. 10, No. 4, pp. 10083-10101, Dec. 2024.: https://doi.org/10.1109/TTE.2024.3381167.

[26] Y. Hakmi, H. Miloudi, M. Miloudi, A. Gourbi, M.H. Bermaki, Frequency experimental identification approach for single-phase induction motor common-mode parameters, *Electrical Engineering & Electromechanics*, Vol. 6, pp. 3–10, 2024. https://doi.org/10.20998/2074-272X.2024.6.01.

[27] A. Gourbi, M. Miloudi, H. Miloudi, M. H. Bermaki, Comparative analysis of differential-mode impedance in single-phase induction motors, *WSEAS Transactions on Circuits and Systems*, Vol. 23, 2024, pp. 261–273. https://doi.org/10.37394/23201.2024.23.26.

[28] S. Dickmann; S. Schenke, Common Mode and Differential Mode Characteristics of AC Motor for EMC Analysis, *International Symposium on Electromagnetic Compatibility – EMC EUROPE* 2016, September 5–9, 2016, Wroclaw, Poland. https://doi.org/10.1109/EMCEurope.2016.7739260

[29] Abdelber B, Med M., Réduction des perturbation électromagnétique conduites dans la machine asynchrone. Mediterranean Journal of Modeling and Simulation Vol. 2, No. 1, 2014, pp.8 -15.

[30] M. Naima, A. Bendaoud, M. Miloudi, H. Miloudi, A. Gourbi, H. Bermaki, Characterizing radiated electromagnetic interference from a power converter for improved electromagnetic compatibility, *WSEAS Transactions on Circuits and Systems*, Vol. 24, 2025, pp. 135–148. https://doi.org/10.37394/23201.2025.24.16.

[31] C. Zhang, J. Jasni, M. A. M. Radzi, N. Azis and X. He, "Research and analysis of electromagnetic interference of a motor drive control system based on PMSM with SiC MOSFET for new energy electric vehicles," Frontiers in Energy Research, Vol. 11, 1338212, 2024, pp.1-13. https://doi.org/10.3389/fenrg.2023.1338212.

[32] D. Stepins, Conducted EMI of switching frequency modulated boost converter, *Electr. Control Commun. Eng.*, vol. 3, no. 1, pp. 12–18, 2013. doi: https://doi.org/10.2478/ecce-2013-0009

[33] M. Pustovetov, Testing of electric drive with a serial connection of the same phases of two induction motors through computer simulation, *WSEAS Transactions on Circuits and Systems*, Vol. 22, 2023, pp. 152–157. https://doi.org/10.37394/23201.2023.22.17.

[34] A. Bouklata, S. Barbara, M. Benyassi, H. Oubouaddi, C. Abdelaali, A. Brouri, Adaptive nonlinear states observer design of switched reluctance machine, *WSEAS Transactions on Circuits and Systems*, Vol. 24, 2024, pp. 105–111. https://doi.org/10.37394/23201.2025.24.12.

[35] S. Bediar, H. Glaoui, R. Dehini, Analysis of the electromechanical behavior of a double-star induction motor with rotor bar faults, *WSEAS Transactions on Systems and Control*, Vol. 20, 2025, pp. 288–295. https://doi.org/10.37394/23203.2025.20.32.

[36] K. K. Chittibabu and N. K. Alphonse, Analysis of conducted EMI with a standalone solar-powered DC motor, *Turk. J. Electr. Eng. Comput. Sci.*, vol. 21, no. 5, pp. 1260–1271, 2013. https://doi.org/10.3906/elk-1110-7

[37] Z. Boussada, B. Omri, M. Ben Hamed, Stator flux orientation control of induction motor fed by three-level NPC inverter, *WSEAS Transactions on Systems and Control*, Vol. 20, 2025, pp. 239–246. https://doi.org/10.37394/23203.2025.20.26.

[38] J. Vissio, A. García, Dynamic model simulations using real world measurements in a wind power generator, *WSEAS Transactions on Systems and Control*, Vol. 20, 2025, pp. 262–267. https://doi.org/10.37394/23203.2025.20.29.

[39] H. Loschi, R. Smolenski, P. Le żynski, D. Nascimento, G. Demidova, Aggregated Conducted Electromagnetic Interference Generated by DC-DC Converters with Deterministic and Random Modulation, *Energies*, Vol. 13, No. 14, 2020, pp.1-9. https://doi.org/10.3390/en13143698

[40] A. Gourbi, M. Miloudi, M. Brahami, Analysis of hybrid photovoltaic system performance, *Advances in Green Energies and Materials Technology*, 2021, pp. 279–286. https://doi.org/10.1007/978-981-16-0378-5_37.

[41] L. Zhai, L. Lin, X. Zhang, and C. Song, The effect of distributed parameters on conducted EMI from DC-fed motor drive systems in electric vehicles, *Energies*, vol. 10, no. 1, pp. 1–17, 2017. https://doi.org/10.3390/en10010001

[42] Fatima T, Rabbeh O., Study and Design of a Plasma Reactor Using a Porous Dielectric Barrier, *The Eurasia Proceedings of Science, Technology, Engineering and Mathematics*, Vol. 38, 2025, pp. 257-263. https://doi.org/10.55549/epstem.1223.

[43] Samira Bediar, Hachemi Glaoui, Rachid Dehini, Analysis of the Electromechanical Behavior of a Double-Star Induction Motor with Rotor Bar Faults, *WSEAS Transactions on Systems and Control*, Vol. 20, pp. 288-295, 2025, Article 201. https://doi.org/10.37394/23203.2025.20.32

[44] Hireche Slimane, Mohamed Habbab, Abdeldjebar Hazzab, Ahmed Khalil Moussaoui, Ambrish Chandra, Hicham Gouabi, Alhachemi Moulay Abdellah., Fault diagnosis decentralized of manufacturing systems using Boolean models. *International Journal of Power Electronics and Drive Systems*, Vol. 14, No. 4, pp. 2700-2708, 2024. https://doi.org/10.11591/ijpeds.v15.i4.pp2700-2708.

[45] A. Ait Salih, Z. M'barki, Y. Mejdoub, K. Senhaji Rhazi, Black-box Modelling of Electromagnetic Compatibility in DC-DC Converters for Electric Vehicles, *Acta IMEKO*, Vol. 14, No. 2, 2025, pp. 1–8. DOI: https://doi.org/10.21014/actaimeko.v14i2.2035.

[46] C. L. Fortescue, Method of symmetrical coordinates applied to the solution of polyphase networks, *Transactions of the American Institute of Electrical Engineers*, Vol. 37, 1918, pp. 1027–1140.

Contribution of Individual Authors to the Creation of a Scientific Article (Ghostwriting Policy)

The authors equally contributed in the present research, at all stages from the formulation of the problem to the final findings and solution.

Sources of Funding for Research Presented in a Scientific Article or Scientific Article Itself

No funding was received for conducting this study.

Conflict of Interest

The authors have no conflicts of interest to declare.